Journal of Photochemistry & Photobiology, B: Biology 168 (2017) 30–39

Contents lists available at ScienceDirect

Journal of Photochemistry & Photobiology, B: Biology

journal homepage: www.elsevier.com/locate/jphotobiol

Low-level laser therapy (LLLT) accelerates the sternomastoid muscle regeneration process after myonecrosis due to bupivacaine

Cristiane Neves Alessi Pissulin [a,b,*], Ana Angélica Henrique Fernandes [c], Alejandro Manuel Sanchez Orellana [d], Renata Calciolari Rossi e Silva [e], Selma Maria Michelin Matheus [f]

[a] Department of Anatomy, Universidade do Oeste Paulista (UNOESTE), Presidente Prudente, SP, Brazil
[b] General Bases of Surgery, Botucatu Medical School, Unesp, Botucatu, SP, Brazil
[c] Department of Chemistry and Biochemistry, Institute of Bioscience, Unesp, Botucatu, SP, Brazil
[d] Unesp, Institute of Bioscience, Botucatu, SP, Brazil
[e] Department of Pathology, Universidade do Oeste Paulista (UNOESTE), Presidente Prudente, SP, Brazil
[f] Department of Anatomy, Institute of Bioscience, General Bases of Surgery, Botucatu Medical School, Unesp, Botucatu, SP, Brazil

ARTICLE INFO

Article history:
Received 8 September 2016
Accepted 19 January 2017
Available online 26 January 2017

Keywords:
Bupivacaine
Low-level light therapy
Muscle regeneration
Fibrosis

ABSTRACT

Background: Because of its long-lasting analgesic action, bupivacaine is an anesthetic used for peripheral nerve block and relief of postoperative pain. Muscle degeneration and neurotoxicity are its main limitations. There is strong evidence that low-level laser therapy (LLLT) assists in muscle and nerve repair. The authors evaluated the effects of a Gallium Arsenide laser (GaAs), on the regeneration of muscle fibers of the sternomastoid muscle and accessory nerve after injection of bupivacaine.

Methods: In total, 30 Wistar adult rats were divided into 2 groups: control group (C: n = 15) and laser group (L: n = 15). The groups were subdivided by antimere, with 0.5% bupivacaine injected on the right and 0.9% sodium chloride on the left. LLLT (GaAs 904 nm, 0,05 W, 2.8 J per point) was administered for 5 consecutive days, starting 24 h after injection of the solutions. Seven days after the trial period, blood samples were collected for determination of creatine kinase (CK). The sternomastoid nerve was removed for morphological and morphometric analyses; the surface portion of the sternomastoid muscle was used for histopathological and ultrastructural analyses. Muscle CK and TNFα protein levels were measured.

Results: The anesthetic promoted myonecrosis and increased muscle CK without neurotoxic effects. The LLLT reduced myonecrosis, characterized by a decrease in muscle CK levels, inflammation, necrosis, and atrophy, as well as the number of central nuclei in the muscle fibers and the percentage of collagen. TNFα values remained constant.

Conclusions: LLLT, at the dose used, reduced fibrosis and myonecrosis in the sternomastoid muscle triggered by bupivacaine, accelerating the muscle regeneration process.

1. Introduction

Local anesthetics are generally used in clinical, medical and dental practices to reduce operative pain [1–7]and as co-adjuncts in postoperative analgesia [8–13].

Many adverse effects have been reported as a consequence of the injection of local anesthetics; these include numbness, muscle weakness [14,15], lockjaw [16,17], inflammation [18], paresthesia [15] and muscle degeneration [19–22].

In the potentiality hierarchy of local anesthetics, bupivacaine is believed to be neurotoxic [21,23,24], and the most myotoxic [25], leading to the formation of scar tissue, multiple calcifications in muscle tissue [26],myonecrosis and acute degeneration [19,22,27–29].

Considering these alterations, bupivacaine has also been used in experimental protocols as a model for myonecrosis [20–22] as well as for the characterization of denervation [19].

Used for epidural and spinal anesthesia, bupivacaine is considered a long-lasting local anesthetic, having the potential to trigger medical complications such as cauda equina syndrome, permanent spinal nerve injury, edema, vacuolization and breaks in the myelin sheath; degeneration of neurons and nuclei fragmentation [21,23,24,30], transient neurologic syndrome [31], and neuronal apoptosis [21,23,24,30,32–34].

Laser therapy (LT) has been reported to play a positive role in muscle regeneration. LT acts as an analgesic, stimulating the proliferation of

* Corresponding author at: Departamento de Anatomia, Faculdade de Odontologia, Rua José Bongiovanni, 700, Cep 18050-680, Unoeste, Campus I, Presidente Prudente, SP, Brazil.
E-mail addresses: crispissulin@gmail.com (C.N. Alessi Pissulin), angelica@ibb.unesp.br (A.A. Henrique Fernandes), alesanc96@outlook.com (A.M. Sanchez Orellana), renata@unoeste.br (R.C. Rossi e Silva), micmath@ibb.unesp.br (S.M. Michelin Matheus).

http://dx.doi.org/10.1016/j.jphotobiol.2017.01.021
1011-1344/

muscle and satellite cells, enhancing protein synthesis in myoblasts and increasing the area of muscle fibers and mitochondrial density [35–42]. Laser irradiation also acts as an adjunctive therapy in neuronal injury [43] and chronic pain relief [44–45]. It reduces myonuclear apoptosis and myogenic cells resulting from musculoskeletal disorders [46].

Because local anesthetics are of fundamental importance in clinical practice and the deleterious effects of bupivacaine on muscle and nerve tissue are well described in the literature. LLLT emerges as a non-invasive co-adjunctive procedure to minimize tissue damage, which is a potential complication in clinical practice.

The objective of the present study was to investigate the effects of low-level laser therapy on the healing process of muscle fibers of the sternomastoid muscle and accessory nerve after injection of bupivacaine.

2. Methodology

Thirty adult male Wistar rats were kept in individual cages with food and water ad libitum in an environment with controlled temperature (24 ± 2 °C) and photoperiod (12 h:12 h). All experiments and procedures were approved by the Animal Use Ethics Committee (São Paulo State University, UNESP, CEUA - Protocol 509).

The animals were anesthetized with ketamine/xylazine (90 mg/kg and 10 mg/kg, respectively) intraperitoneally. A midline incision was performed on the ventral side of the neck to expose the sternomastoid muscles. The injections were then administered as follows: 0.05 ml bupivacaine hydrochloride (5 mg/ml) (HypoFarma) in the right antimeres and sodium chloride 0.9% in the left antimeres; the skin was sutured with n° 3.0 black nylon (Brasutura®). The solutions were deposited in the open muscle field, subfascially in the middle third [47] and distal muscle portion [48].

After 24 h, the animals were randomly divided into two groups: control and laser.

The laser group received laser treatment during 5 consecutive days with a GaAs diode laser (Endophoton, KLD Biosystems, Amparo, Brazil) with a pulsed emission wavelength of 904 nm, radiant power of 0.05 W (50 mW), pulse frequency of 10.000 Hz, pulse duration of 100 ns, duty cycle of 0.1%, peak radiant power of 50 W, spectral bandwidth of 5%, divergent beam profile (8° × 25°), and spot size of 0.035 cm^2. This wavelength of 904 nm was used to obtain a greater depth of penetration, recommended for deep lesions [42].

The previously calibrated laser was directly applied to the skin (direct contact) in the injection areas in both antimeres. The application was performed with the laser pen held at an angle of 90° to the irradiated surface. The delivery per point presented energy density of 69 J/cm^2, corresponding to treatment for 48 s (seconds), irradiance was 1.42 W/cm^2, and radiant energy of 2.4 J. The final total radiant energy was 4.8 J. The irradiation time and final energy were automatically controlled by the previously calibrated laser equipment.

Four groups were formed based on antimeres and treatment: right antimeres - CBupi (without LLLT), LBupi (with LLLT); left antimeres CCl (without LLLT), LCl (with LLLT).

Seven days after application of the solutions, the animals were anesthetized with ketamine/xylazine (90 mg/kg and 10 mg/kg, respectively) intraperitoneally and then decapitated. Blood samples were collected, centrifuged at 936 RCF, and the plasma was frozen.

The sternomastoid muscle used in this study consisted of two macroscopically clearly distinguishable even portions, white and red [49]. Based on the bupivacaine diffusion, only the superficial muscle portions were removed with the associated nerve and processed for analyses.

2.1. Creatine kinase (CK)

Serum samples and approximately 100 mg of muscle tissue were used from each group ($n = 5$ in each group) for the determination of creatine kinase activity (Kit Labtest – CK-nac liquiform 117-1/60) [50].

The absorbance of the samples was read at 25 °C using a UV spectrophotometer with a wavelength of 340 nm and quartz cells with a 1-cm optical path length.

2.2. Histopathological analysis of muscle tissue and collagen quantification

Fragments of the surface portion of the sternomastoid muscle ($n = 5$) after being frozen in liquid nitrogen (−170 °C) were sectioned (6 μm) in a Leica CM1800 cryostat (−25 °C). Two slides were prepared; the first was stained with Hematoxylin-Eosin (HE) and the second with Picrosirius Red [51]. The slides stained with HE were analyzed using a photomicroscope (BX 41-2) with a digital camera (model SIS-SC30) and objectives of 20× and 40× for image capture. Double-blind semi-quantitative analysis of the degree of tissue components (inflammatory infiltrate, atrophy and necrosis) was described as absent (grade 0), mild (grade 1), moderate (grade 2) and high (grade 3) [52]. These images were also used to count the central and peripheral nuclei with the "Image J" software program (http://rsbweb.nih.gov/ij/).

To quantify intramuscular collagen, 5 random images of each slide were obtained (20×). The percentage of collagen was calculated using Leica QWin software (Wetzlar, Germany).

2.3. Transmission Electron Microscopy (TEM)

Muscle fragments ($n = 5$ in each group), fixed in Karnovsky solution, were processed according to the routine for Transmission Electron Microscopy analysis by the Electron Microscopy Center IB/Unesp/Botucatu. Ultra-thin sections were obtained from longitudinal cuts in muscle fragments using an ultramicrotome (Ultratome 880 LKB III) and stained with uranyl acetate solution in 50% alcohol and subsequently with lead citrate. The material was analyzed and photographed with a transmission electron microscope (TECNAI Spirit Fei Company).

2.4. Morphological and morphometric analyses of the sternomastoid nerve

Sternomastoid nerve fragments ($n = 5$ in each group), after fixation in Karnovsky solution, were post-fixed in osmium tetroxide 1%. Twenty-four hours later, the histological routine was performed, during which cross sections were obtained (6 μm) and histological slides were prepared. For each experimental group, 100× images were obtained with immersion oil in the photomicroscope (Axiophot–2) using a digital camera (model AxioCam HR, Zeiss). The following variables were measured: number of axons, axonal diameters (Σ axon diameter / number of axons) and nerve fibers (Σ fiber diameter / number of fibers). The following calculations were performed with the free software "ImageJ" (http://rsbweb.nih.gov/ij/): thickness of the myelin sheath (fiber diameter − diameter of axon / 2) and G-ratio (average diameter of axons / average diameter of nerve fibers).

2.5. Western blotting

Frozen muscle samples (third medium)from 5 animals from each group were homogenized with a tissue homogenizer (IKA UltraTurrax/T-25) in 0.5 ml of lysis buffer (1% Triton X-100, 10 mM sodium pyrophosphate, 100 mM sodium fluoride, aprotinin 10 μg/ml, 1 mM PMSF, sodium orthovanadate - 0.25 mM Na_3VO_4, 150 mM NaCl and 50 mM Tris-HCl, pH 7.5). The samples were centrifuged at 11,000 rpm for 20 min and the supernatant collected. A 100-μL aliquot of the homogenate was treated with 100 μL of Laemmli sample buffer (2% SDS, 20% glycerol, bromophenol blue 0.04 mg/ml, 0.12 M Tris-HCl, pH 6.8, and 0.28 M β-mercaptoethanol). The samples were then incubated at 97 °C for 5 min and stored in a freezer at −20 °C until use.

One aliquot of the pure extract from each sample (not treated with Laemmli) was used to quantify total protein using the Bradford method (Bradford, 1976). Exact quantities of the total protein from each sample (70 μg) were subjected to electrophoresis in 4–15% polyacrylamide gel

(SDS-PAGE) and then transferred to nitrocellulose membranes (Bio-Rad Laboratories, Hercules, California) in the wet system.

The proteins transferred to the membranes were blocked with 5% skimmed milk diluted in TBS-Tween for 1 h at room temperature and incubated with different TNFα primary antibodies (Abcam – ab66579; 1 mg/ml) (Gapdh – Cell Signaling - 14C10; 1:1000), overnight at 4 °C. After incubation with the primary antibody, the membranes were washed in TBS-Tween and incubated with specific *anti*-rabbit secondary antibody (Cell Signaling - 7074 s) 1:5000 for 1 h at room temperature. Again, the membranes were washed, and the ECLTM Selected Western Blotting Detection Reagent (GE Healthcare, Uppsala, Sweden) detection system was used. After image capture in a transilluminator G-Box, densitometric quantification of the bands was performed using Image J software (version 1.71, 2006, Austria). The protein expression values were normalized to the values obtained for the GAPDH protein, which was used as a reference.

2.6. Statistical analysis

The data were expressed as mean and standard deviation (the diameters of the axons and the fibers, the thickness of the myelin sheath, the G-ratio, the percentage of collagen), and as average and minimum and maximum values (the number of the axons, the number of central and peripheral nuclei and the TNFα protein expression). Values with $p \leq 0.05$ were considered statistically significant. The Shapiro Wilk test was used to the normality of the data. The number of the axons and the central and peripheral nuclei were subjected to the Kruskal Wallis followed by Dunn Test. The axons and fibers diameters, thickness of the myelin sheath, G-ratio, percentage of collagen and TNFα protein expression were evaluated by ANOVA with Bonferroni correction for multiple comparisons [53].

3. Results

Macroscopically, 7 days after the application of bupivacaine, a decrease in muscle volume was observed in the control group that received bupivacaine, compared to the control group that received sodium chloride (Fig. 1A). After LLLT treatment, the muscle volume approached to normal, suggesting regeneration (Fig. 1B).

3.1. Creatine kinase (CK)

The results of the quantification of CK serum levels revealed no statistically significant differences between the groups: Control (216.69 ± 30.54) and Laser (205.63 ± 40.50), $p > 0.05$.

We observed that muscle CK levels were higher in the control group that received bupivacaine (401.55 ± 40.41) compared to the group that received sodium chloride (331.90 ± 41.51), $p < 0.01$. After laser therapy, there was a statistically significant decrease in CK levels (310.20 ± 38.51) ($p < 0.01$).

3.2. Histopathological, electron micrograph, and quantification of collagen and western blot analyses

The general morphological analysis of the sternomastoid muscles stained with HE demonstrated the presence of inflammatory cells with basophilic nuclei (mononuclear cell infiltration), blood vessels with hyperemia, edema in the connective tissue, muscle fibers in a degenerative and necrotic process and total loss of its polygonal characteristic in the control group that received bupivacaine (Fig. 2Aa). When it was possible to identify the muscle fibers, central nuclei were associated. After laser application, a lower quantity of inflammatory infiltrate was observed; areas in the process of regeneration were present, characterized by the presence of muscle fibers with basophilic cytoplasm containing central and peripheral nuclei (Fig. 2Ab).

In the control group that received sodium chloride, there was loss of the polygonal characteristic in only a few muscle fibers; the mononuclear cell infiltration was slight when compared to the group that received bupivacaine (Fig. 2Ae). After application of LLLT, the presence of inflammatory infiltrate was not detected and the histological architecture of the muscle fibers was preserved (Fig. 2Af). The presence of fibroblasts in the endomysium of the animals that received LLLT in both antimeres was common.

The double-blind semi-quantitative analysis confirmed the histological observations that the muscles of the control group that received bupivacaine had significantly higher scores related to inflammation, atrophy and necrosis. When the anesthetic was associated with laser treatment, an attenuation of general pathological processes was observed. In the control group that received sodium chloride, only minor alterations were observed with regard to inflammation; after application of LLLT, there were no alterations (Table 1) (values in scores).

There was an increase in the quantification of central nuclei in the control group that received bupivacaine (277) ($p < 0.01$) and a decrease in the number of peripheral nuclei [53] ($p < 0.05$) compared to the groups that received sodium chloride (Fig. 2B e C). In the group that received bupivacaine and LLLT, there was a statistically significant increase in the number of peripheral nuclei (287) ($p < 0.05$) (Fig. 2C).

The evaluation of TNFα protein expression in all experimental groups revealed no statistically significant differences, although a decrease in TNFα expression was observed in the group receiving bupivacaine and LLLT application (Fig. 2D).

The ultrastructural analysis found comparatively normal myofibrils, without signs of alteration, Z rectilinear line, inter-myofibrillar mitochondria of varying sizes and T tubules associated with the cisternae of the sarcoplasmic reticulum forming triads in the group that received sodium chloride (Fig. 2Ag and Ah).

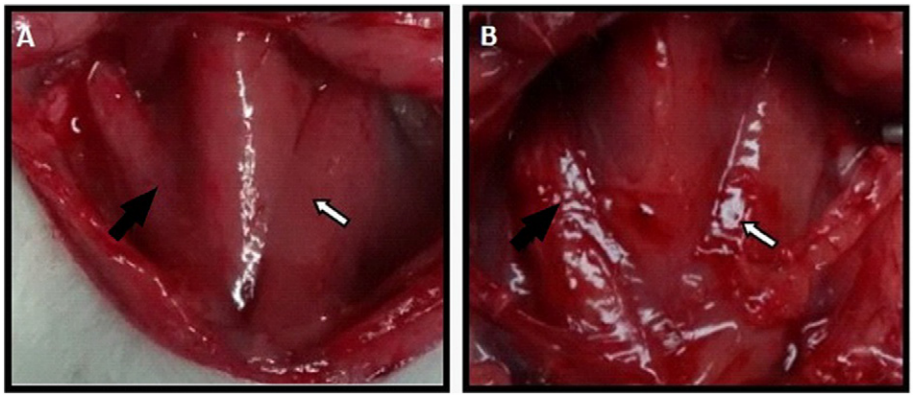

Fig. 1. Ventral view of the right and left sternomastoid muscles. After 7 days of bupivacaine and chloride injections (A) CBupi (➡) and CCl (⇨); and applying LLLT, (B) LBupi (➡) and CCl (⇨).

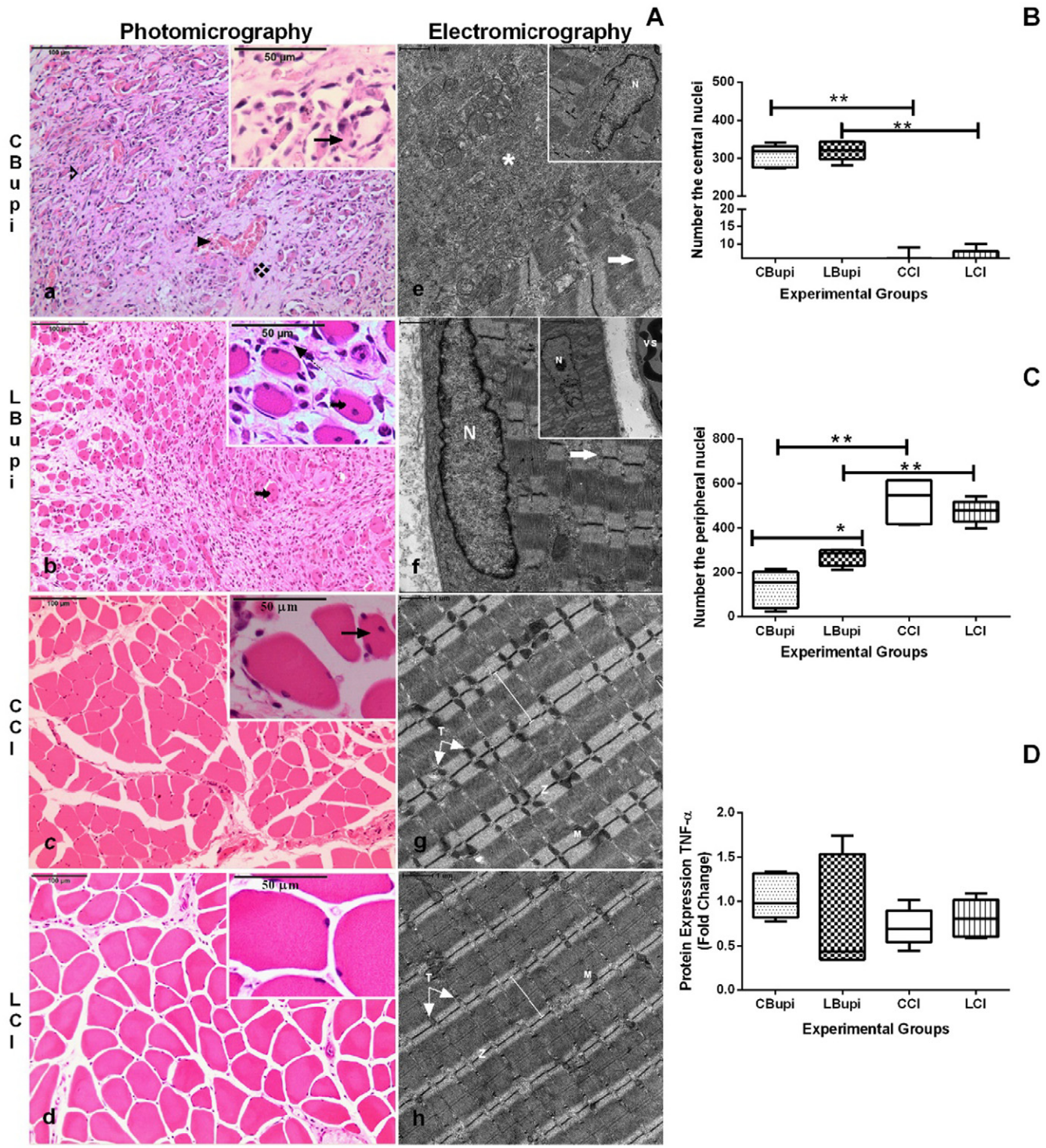

Fig. 2. A - Photomicrography and electromicrography of cross sections of the sternomastoid muscle from the Control and Laser groups (HE). (a) The presence of mononuclear cell infiltration (▸), edema (✣), blood vessels with hyperemia (▶), muscle fibers in a degenerative process, necrotic and with total loss of polygonal characteristic (➞). (b) Muscle cells in the process of regeneration (➠), and fibroblasts (⇢). (c) Partial loss of the polygonal characteristic of the muscle fibers (➞). (d) Muscle fibers with preserved histological architecture. Electromicrography: mitochondria (m), Z line (Z), triads (T), sarcomeres ([). e: areas in regeneration (*), nuclei (N), areas of myonecrosis (*), normal myofibrils (white arrows). F: blood vessels (VS). B - Quantification of the number of central nuclei in the subgroups. CBupi: 319(275,342); LBupi: 321(282,345); CCl: 3(1,9); LCl: 6(1,10). C - Quantification of the number of peripheral nuclei in the subgroups. CBupi: 152(22,216); LBupi: 287(215,302); CCl: 547(417,616); LCl: 479(398,542). $p < 0.05$; $^{**}p < 0.01$. D - Protein expression of TNFα through western blot of the CBupi: 0.986(0.778,1.336), LBupi: 0.442(0.347,1.743), CCl: 0.696(0.447,1.016), LCL: 0.811(0.591,1.092). The data are represented in average (boxes) and minimum and maximum values (whiskers).

In the group that received bupivacaine, degeneration regions and myonecrosis were present, containing disorganized myofibrils with fragmented and discontinuous Z line and abundant central nuclei. Inflammatory cells, areas of fibrosis and signs of edema were present (Fig. 2Ae).

After application of LLLT, organized sarcomeres and scarce degeneration regions were detected. The nuclei were for the most part peripheral, and blood vessels and central nuclei were present (Fig. 2Af).

The Red Picrosirius coloring enabled analysis of the collagen fibers present in the endomysium and perimysium, which were marked in

Table 1
Morphological comparison of general pathological processes in experimental models exposed to bupivacaine and the laser.

Subgroups	N (%)	General pathological processes - Med (Vmin — Vmax)		
		Inflammation	Atrophy	Necrosis
CBupi	5,0 (25)	2,0 (2,0–3,0)[1]	2,0 (1,0–2,0)[2]	2,0 (2,0–3,0)[3]
CCl	5,0 (25)	1,0 (0,0–0,0)	1,0 (0,0–1,0)	0,0 (0,0–0,0)
LBupi	5,0 (25)	1,0 (0,0–2,0)	1,0 (0,0–1,0)	0,0 (0,0–0,0)
LCl	5,0 (25)	1,0 (1,0–1,0)	0,0 (0,0–0,0)	0,0 (0,0–0,0)
Total	20,0 (100)			

Legends: Scores semiquantitative general disease processes in experimental models. Med = median; Vmin = minimum value; Vmax = maximum value. Significant values: [1]p = 0.009; [2]p = 0.008; [3]p = 0.008, [52].

red, and the muscle fibers in yellow. This analysis was performed using conventional optical light microscopy and optical polarized light microscopy (Fig. 3A). In the group that received sodium chloride, an increase in red tone staining was identified in polarized light, suggesting the presence of mature collagen - type I. In the bupivacaine group, the birefringence of collagen fibers tended from yellow to green, suggesting the presence of type III collagen fibers (newly synthesized) (Fig. 3A).

The analysis revealed that the percentage of collagen increased in the area of fibrosis in the group that received bupivacaine (53.3 ± 8.2) compared to the group that received sodium chloride (17.08 ± 6.0) ($p < 0.05$). After the laser treatment, there was a reduction in the area of fibrosis in both the groups that received bupivacaine (24.19 ± 8.66) and those that received sodium chloride (14.11 ± 1.16) ($p < 0.01$) (Fig. 3B).

3.3. Morphological and morphometric analyses of the sternomastoid nerve

For the doses of 0.5% bupivacaine and 0.9% sodium chloride, in all groups, the histological images of the sternomastoid nerves demonstrated axon and intact myelin sheath, and axoplasm and endoneurium with morphology within the normal range. The ultrastructural analysis revealed bundles of organized myelinated axons containing neurofilaments and integral and concentric myelin sheaths without signs of demyelination. The axolemma and Schwann cells (represented by the nucleus) were well preserved. The endoneurium contained collagen cells oriented longitudinally (Fig. 4A).

The morphometric analyses of the number of axons, diameters of axons and nerve fibers, as well as calculations of the thickness of the myelin sheath and the G ratio, showed no statistically significant differences between the groups ($p < 0.05$) (Figs. A, B, C, D). The G-ratio demonstrated values of approximately 0.5, consistent with normal nerves (Fig. 4E).

4. Discussion

The results of the present study suggest that the bupivacaine dose used (0.5%) caused myonecrosis. It was observed increases in muscle CK ($p < 0.05$) and scores related to inflammation, atrophy and necrosis. No morphological alterations related to the neurotoxic effect of the anesthetic were observed, and the G-ratio values were within the normal range (0.5), although several studies in the literature have described the presence of neurotoxic effects associated with the anesthetic bupivacaine [15,23,54].

The lower G-ratio values (near 0.4) indicate degeneration of the axon, while high values (near 0.7) indicate myelin degeneration or regeneration [55]. Some neurological lesions was observed in the root and posterior column of the spinal cord after intrathecal anesthesia with bupivacaine, along with ultrastructurally identified edema, vacuolation of the myelin sheath, neuronal apoptosis and disruption of the myelin sheath [23].

Long-acting bupivacaine produces morphological alterations similar to muscular atrophy [56], as demonstrated in studies on denervation [19,27,57].

Myonecrosis caused by bupivacaine is due to excessive intake of intracellular Ca^{2+} ions, which promotes the activation of proteases, resulting in sarcomere disruption [56]. This framework is observed ultrastructurally through disorganized myofibrils, a fragmented and discontinued Z line, abundant central nuclei, the presence of inflammatory cells, and areas of fibrosis and edema. Due to the excessive accumulation of Ca^{2+}, there are alterations in the morphology and function of the mitochondria, which trigger inhibition of enzymatic activity and block the synthesis of ATPase, resulting in myonecrosis [58,59].

Among the parameters used to verify myonecrosis, the CK level is commonly used in the diagnosis of myopathies [60–63]. In the experimental control and laser groups ($p > 0.05$), no changes were found in serum CK levels. The increased muscle CK levels after administration of bupivacaine suggested a local and non-systemic effect of the anesthetic. Cereda et al. [64] observed a 5.5-fold increase in serum CK levels after injection with plain formulations of bupivacaine.

On the other side a reduction in serum CK was present after 5 sessions of laser therapy (810 nm) with a final energy of 4.8 J in water polo athletes [65].

After LLLT, it was observed a decrease in muscle CK ($p < 0.01$). Decreases in CK values are directly related to the reduction in myonecrosis described after laser therapy [64,66], which has been used for its anti-inflammatory, regenerative and analgesic actions [35,42,65]. CK is an enzyme associated with the formation of ATP, found primarily in skeletal and cardiac muscle and in the brain. It catalyzes the reversible phosphorylation of creatine into phosphocreatine with the release of adenosine triphosphate (ATP) from high energy phosphate. In muscle tissue, phosphocreatine acts as an energy storage molecule, and in cases of energy needs, a cleavage is performed to supply ATP for muscle activity [60]. After LLLT, the mitochondrial metabolism is modulated, promoting an increase in ATP synthesis as a secondary response [67].

The treatment with the GaAs laser used in this study (904 nm) with high final energy of 4.8 J, applied for 5 consecutive days, was also able to reduce inflammation and atrophy, as well as the number of central nuclei and the percentage of collagen. Ultrastructurally, after the LLLT, the sarcomeres were for the most part arranged, and the majority of the nuclei was peripheral. The TNFα values remained constant.

TNFα is a pro-inflammatory cytokine that stimulates other cytokines, acting as a chemotactic agent of inflammatory cells, mainly activated by macrophages in the lesion process, collagen synthesis and production of extracellular matrix proteins [68].

The LLLT acts by inhibiting factors involved in inflammation, such as pro-inflammatory cytokines [69] and its use has been described to be able to decrease the TNFα levels. Mesquita-Ferrari et al. [70] detected a significant decrease in TNF-α mRNA expression in the cryoinjury group after LLLT. Similar results were also observed after six days of LLLT applications after cryoinjury [42]. Even after 4 days of cryolesion and LLLT therapy [71] and after 14 days [72] a decrease in muscle levels of TNF-α was found. Pires et al. [73] studied tendinitis in rats after 7 and 14 days and they showed that LLLT reduced the TNF-α expression only at chronic phase. Macedo et al. [74] studying dystrophic muscle cells verified that LLLT treatment reduced the TNF-α and NF-κB levels. Mantineo et al. [75] utilized LLLT at five frequencies (5, 25, 50, 100, and 200 Hz) for treating inflammation induced in the gastrocnemius muscle and the treatment effects occurred for all doses with a reduction of TNF-α, IL-1β, IL-6 cytokines and inflammatory cells.

Our results related to the TNFα protein expression in all experimental groups revealed no statistically significant differences, although a decrease in TNFα expression was observed in the group LBupi. Probably it has been one limitation of this study. The MDD (minimum detectable difference) was calculated and the result was 0.509 and the greatest difference our study obtained was 0.336 between the groups. Due to a reduced number of samples used in each experimental group, a large

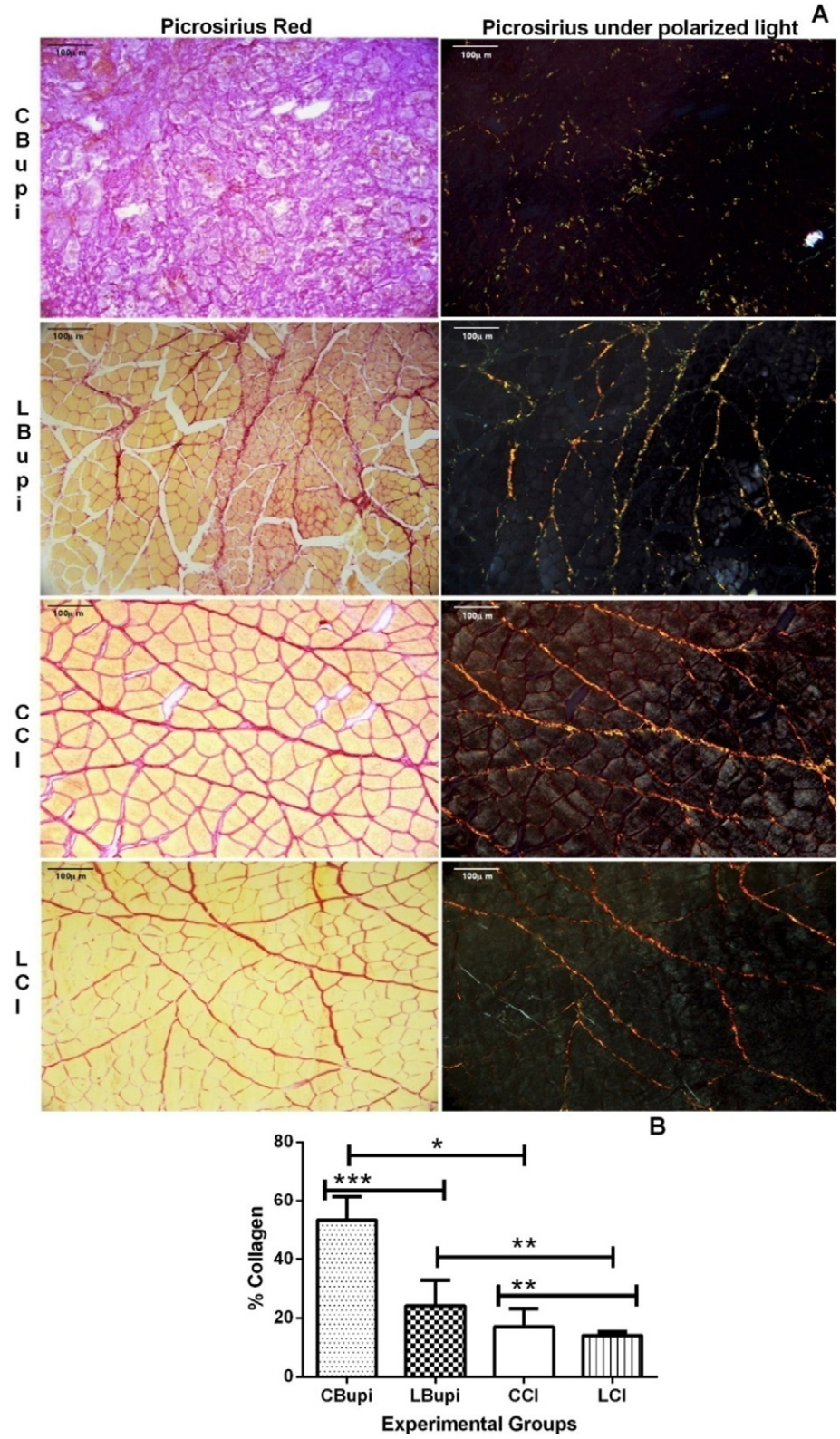

Fig. 3. A - Photomicrographs of cross sections of the sternomastoid muscle (Picrosirius Red). B - Mean (boxes) and standard deviation (whiskers) of collagen area percentages. $^{*}p < 0.05$; $^{**}p < 0.01$; $^{***}p < 0.001$.

dispersion was found in the LBupi group. Maybe this fact could be responsible for the lack of differences observed in the TNFα values.

The quantification of collagen in the present study showed that the area of fibrosis observed in the LBupi subgroup was significantly smaller than in the CBupi group. These data was confirmed by the others studies, in which irradiation with the AsGaAl laser (635 nm, 7 mW) prevented the formation of fibrotic tissue [76]. Laser therapy inhibits fibrosis and accelerates muscle regeneration [77].

A non-significant reduction was observed in the percentage of collagen using the GaAs laser (904 nm, 50 mW) with final energy of 4.8 J at

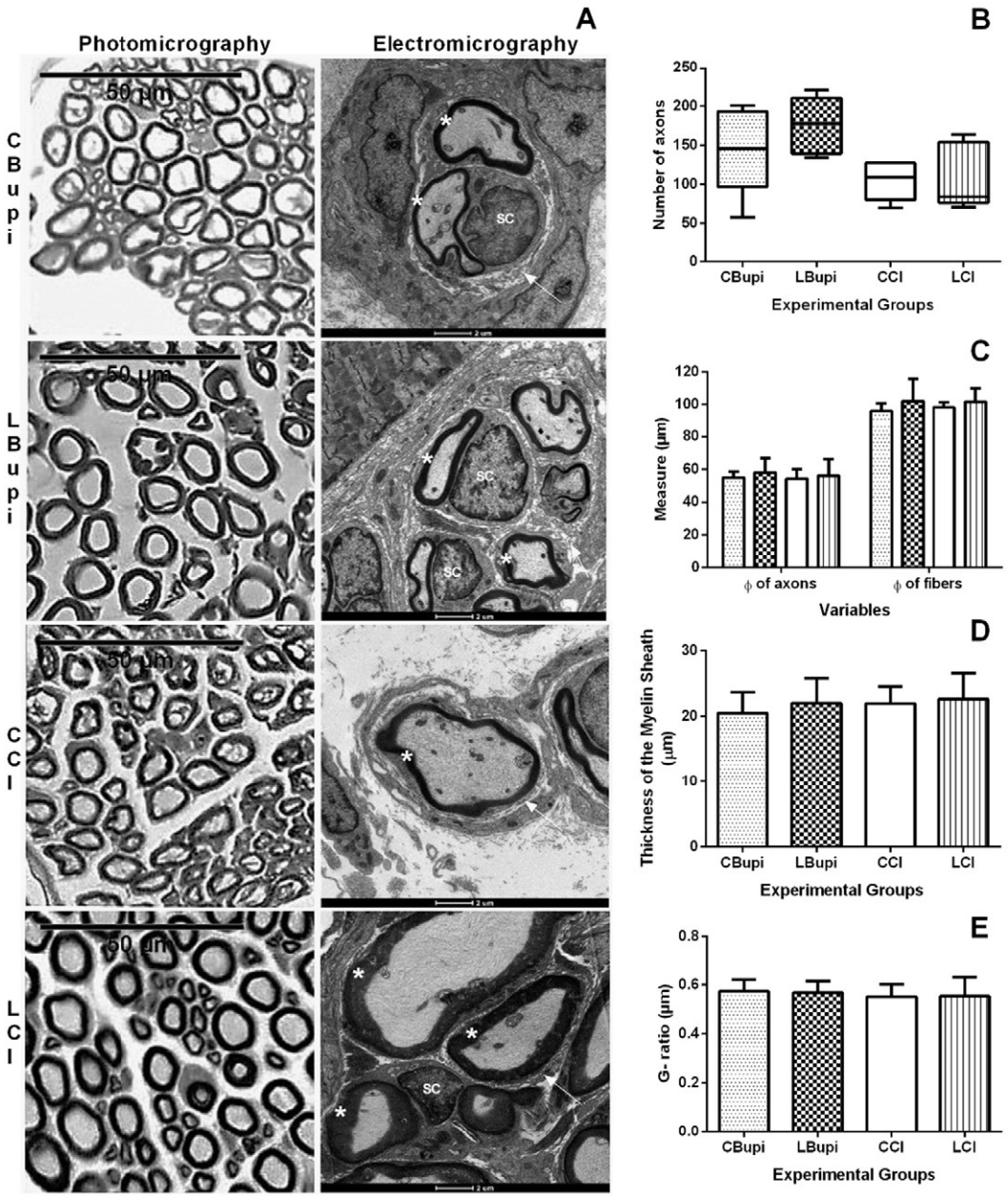

Fig. 4. A - Photomicrographs and electromicrographs of cross sections of the sternomastoid nerves. Schwann Cell Nucleus (SC), myelin sheaths (*), endoneurium (arrow). B - Averages (boxes), minimum and maximum values (whiskers) of the axon numbers. C - Analysis of the axon and fiber diameters. D - Thickness of the Myelin Sheath. E - G ratio of myelinated fibers. The results showed in C, D and E represent the mean (boxes) and the standard deviation (whiskers).

7 days after cryoinjury of the tibialis anterior muscle [42]. Several authors have described an improvement in collagen synthesis and organization after laser therapy [76,78–81].

The integrity of the extracellular matrix promotes support, protection and stabilization of muscle fibers [82]. LLLT remodels the extracellular matrix [81] and TNF-α protein levels during the acute phase of injury, which modulates inflammation [65,83].

After GaAs laser therapy (904 nm), we observed a macroscopic reduction in atrophy in the group that received bupivacaine.

Laser therapy used in muscle regeneration promotes the differentiation of new myofibrils, causing recovery in necrotic tissue. After LLLT application (HeNe - 603 nm, 4 mW, 5 or 10 J/cm^2) was observed the regeneration of muscle fibers with preserved myofibrils and well-defined T tubules and sarcoplasmic reticulum [84].

It was Identified a reduction in myonecrosis and edema after LLLT treatment with an AsGaAl (780 nm, power 40 mW, 3.2 J) in the tibialis anterior muscle after cryoinjury [65]. This muscle recovery was also observed after 5 applications using a GaAs laser (904 nm, 50 mW) with a final radiant energy of 4.8 J [42]. These data suggest that LLLT is a co-adjuvant in muscle improvement at low or high final energy by optimizing the tissue repair process [38]. Moreover, LLLT with diodes emitting at infrared promotes positive responses in skeletal muscle because, they reach a skin depth of 2 to 4 cm [40] with a similar response to the laser used in the present study.

As infrared wavelength was used in the application of LLLT, the absorption occurs through the cytochrome *c* oxidase (COX) [67,85], which is the principal chromophore in cells, increasing mitochondrial products such as ATP, NADH, proteins and RNA and a reciprocal increase in oxygen consumption occurs [86]. All of these physiologic modifications induced by LLLT could have stimulated mitochondrial physiology due to lesions caused by the anesthetic, reducing the levels of muscle catabolism and loss of proteins and promoting regeneration and

organization of muscle tissue [87], which may explain the increased number of nuclei observed in the LBupi subgroup in the present study.

It has been reported that the use of LLLT, even before musculoskeletal injury, promotes better, faster and more efficient muscle repair, reducing myonecrosis, inflammatory infiltrate and collagen synthesis [82].

The Laser therapy effects on tissue involve the utilized dose, the results showed here, for GaAs laser, with a higher final energy (4.8 J) is able to improve the muscle regeneration. Similar results showed that this final energy is able to accelerate muscle recovery [42]. The most important parameters in laser therapy that influence the treatment is the final energy radiated, and it is directly related to the peak power of the equipment and radiation time [88]. The wavelength used in this protocol was 904 nm. The wavelength is related to the radiation penetration power in tissue. The molecule that is absorbed can be transferred to another molecule or cell, which can activate or promote chemical reactions in the surrounding tissue [85].

The biological response to laser therapy depends on the choice of the treatment and irradiation parameters, such as the wavelength, device power, beam area, final energy, irradiation time, treatment frequency, application mode and the start of the treatment. One scientific review, reported that the results are often conflicting, due to the choice of when to start treatment, considering that the intervention can act at different stages of tissue repair [81]. All of these parameters are important to obtain a positive effect of laser therapy, although many studies do not report the complete data, which makes replication and reliability of the findings difficult.

Because LLLT is a low-cost, non-invasive therapy that is easy to administer, it can be introduced both before and after surgery, with beneficial effects similar or superior to oral medications given to reduce inflammation and pain.

5. Conclusion

The results demonstrate that the positive effects of LLLT on the muscle repair process are dependent on parameters of irradiation and treatment. Thus, our results support the use of laser therapy as an easy-to-use and low-cost co-adjuvant therapy, reducing the side effects associated with bupivacaine, accelerating the process of muscle regeneration and promoting reductions in myonecrosis and muscle fibrosis.

Competing interests

The authors declare no competing interests.

Research support

This work was supported by FAPESP Grant n° 13/26649-3.

Acknowledgment

PhD. Carlos Roberto Padovani for statistical analyses.

References

[1] B. Cobb, Y. Cho, G. Hilton, V. Ting, B. Carvalho, Active warming utilizing combined IV fluid and forced-air warming decreases hypothermia and improves maternal comfort during cesarean delivery: a randomized control trial, Anesth. Analg. 122 (5) (2016 May) 1490–1497.
[2] N. Kishore, Y.S. Payal, N. Kumar, N. Chauhan, In spinal anaesthesia for cesarean section the temperature of bupivacaine affects the onset of shivering but not the incidence: a randomized control trial, J. Clin. Diagn. Res. 10 (1) (2016 Jan) UC18–UC21.
[3] I. Balga, H. Gerber, X.H. Schorno, F. Aebersold Keller, H.P. Oehen, Bupivacaine crystal deposits after long-term epidural infusion, Anaesthesist 62 (7) (2013 Jul) 543–548.
[4] B.J. Horn, A. Cien, N.P. Reeves, P. Pathak, C.J. Taunt Jr., Femoral nerve block vs periarticular bupivacaine liposome injection after primary total knee arthroplasty: effect on patient outcomes, J. Am. Osteopath. Assoc. 115 (12) (2015 Dec 1) 714–719.
[5] V.V. Jaichandran, R. Raman, L. Gella, T. Sharma, Local anesthetic agents for vitreo retinal surgery: no advantage to mixing solutions, Ophthalmology 122 (5) (2015 May) 1030–1033.
[6] B.M. Ilfeld, E.R. Viscusi, A. Hadzic, H.S. Minkowitz, M.D. Morren, J. Lookabaugh, G.P. Joshi, Safety and side effect profile of liposome bupivacaine (exparel) in peripheral nerve blocks, Reg. Anesth. Pain Med. 40 (5) (2015 Sep–Oct) 572–582.
[7] P. Shapiro, H. Schroeck, Seizure after abdominal surgery in an infant receiving a standard-dose postoperative epidural bupivacaine infusion, AA Case Rep. (2016 Jan 28).
[8] K. Nouette-Gaulain, C. Dadure, D. Morau, C. Pertuiset, O. Galbes, M. Hayot, et al., Age dependent bupivacaine-induced muscle toxicity during continuous peripheral nerve block in rats, Anesthesiology 111 (5) (2009 Nov) 1120–1127.
[9] Abdolhossein-Davoodabadi, M. Reza-Fazel, H. Reza-Vafaei, S. Parviz, Comparison of the effects of intrapleural bupivacaine and morphine on post-thoracotomy pain, Middle East J. Anaesthesiol. 23 (3) (2015 Oct) 267–272.
[10] H.C. Yang, J.Y. Lee, S. Ahn, S. Cho, K. Kim, S. Jheon, J.S. Kim, Pain control of thoracoscopic major pulmonary resection: is pre-emptive local bupivacaine injection able to replace the intravenous patient controlled analgesia? J. Thorac. Dis. 7 (11) (2015 Nov) 1960–1969.
[11] D.E. Beck, D.A. Margolin, S.F. Babin, C.T. Russo, Benefits of a multimodal regimen for postsurgical pain management in colorectal surgery, Ochsner J. 15 (4) (2015 Winter) 408–412.
[12] K.S. Kalchofner Guerrero, I. Campagna, R. Bruhl-Day, C. Hegamin-Younger, T.G. Guerrero, Intraperitoneal bupivacaine with or without incisional bupivacaine for postoperative analgesia in dogs undergoing ovariohysterectomy, Vet. Anaesth. Analg. (2016 Feb 12).
[13] S.W. Yu, A.L. Szulc, S.L. Walton, R.I. Davidovitch, J.A. Bosco, R. Iorio, Liposomal bupivacaine as an adjunct to postoperative pain control in total hip arthroplasty, J. Arthroplast. (2016 Jan 21) (pii: S0883-5403(16)00064-4).
[14] R.J. Hinton, P.C. Dechow, D.S. Carlson, Recovery of jaw muscle function following injection of a myotoxic agent (lidocaine-epinephrine), Oral Surg. Oral Med. Oral Pathol. 59 (3) (1985 Mar) 247–251.
[15] S. Yang, M.S. Abrahams, P.D. Hurn, M.R. Grafe, J.R. Kirsch, Local anesthetic Schwann cell toxicity is time and concentration dependent, Reg. Anesth. Pain Med. 36 (5) (2011 Sep–Oct) 444–451.
[16] T. Renton, D. Adey-Viscuso, J.G. Meechan, Z. Yilmaz, Trigeminal nerve injuries in relation to the local anaesthesia in mandibular injections, Br. Dent. J. 209 (9) (2010 Nov), E15.
[17] G.A. Sanchez, D. Tanaka, G.L. Alonso, Local anesthetics inhibit Ca-ATPase in masticatory muscles, J. Dent. Res. 89 (4) (2010 Apr) 372–377.
[18] B.S. Kürkçüoğlu, M. Dönmez, S. Altinel, S.B. Akinci, F. Saricaoğlu, U. Aypar, Comparison of intraarticular bupivacaine and levobupivacaine injection in rat synovial inflammation, Turk. J. Med. Sci. 44 (4) (2014) 540–545.
[19] E. Çalgüner, R. Gözil, D. Erdogân, I. Kurt, S. Keskil, Ç. Elmas, H. Sabuncuoglu, Atrophic and regenerative changes in rabbit mimic muscles after lidocaine and bupivacaine application, Anat. Histol. Embryol. 32 (2003) 54–59.
[20] D. Danieli-Betto, S. Peron, E. Germinario, M. Zanin, G. Sorci, S. Franzoso, D. Sandonà, R. Betto, Sphingosine 1-phosphate signaling is involved in skeletal muscle regeneration, Am. J. Phys. Cell Physiol. 298 (3) (2010 Mar) C550–C558.
[21] X. Wen, S. Xu, H. Liu, Q. Zhang, H. Liang, C. Yang, H. Wang, Neurotoxicity induced by bupivacaine via T-type calcium channels in SH-SY5Y cells, PLoS One 8 (5) (2013 May 2), e62942.
[22] I. Otrocka-Domagała, A. Mikołajczyk, K. Paździor-Czapula, M. Gesek, T. Rotkiewicz, M. Mikiewicz, Effect of low-energy laser irradiation and antioxidant supplementation on cell apoptosis during skeletal muscle post-injury regeneration in pigs, Pol. J. Vet. Sci. 18 (3) (2015) 523–531.
[23] J. Ji, X. Yan, Z. Li, Z. Lai, J. Liu, Therapeutic effects of intrathecal versus intravenous monosialoganglioside against bupivacaine-induced spinal neurotoxicity in rats, Biomed. Pharmacother. 69 (2015 Feb) 311–316.
[24] J. Kato, J. Konishi, H. Yoshida, T. Furuya, A. Kashiwai, S. Yokotsuka, D. Gokan, S. Ogawa, Caudaequina syndrome following combined spinal and epidural anesthesia: a case report, Can. J. Anaesth. 58 (7) (2011 Jul) 638–641.
[25] L.E. Mather, The acute toxicity of local anesthetics, Drug Metab. Toxicol. 6 (11) (2010) 1313–1332.
[26] W. Zink, G. Missler, B. Sinner, E. Martin, R.H. Fink, B.M. Graf, Differential effects of bupivacaine and ropivacaine enantiomers on intracellular Ca2+ regulation in murine skeletal muscle fibers, Anesthesiology 102 (4) (2005 Apr) 793–798.
[27] P.W. Benoit, W.D. Belt, Destruction and regeneration of skeletal muscle after treatment with a local anesthetic, bupivacaine (Marcaine), J. Anat. 107 (1970) 547–556.
[28] R. Perez-Castro, S. Patel, Z.U. Garavito-Aguilar, A. Rosenberg, E. Recio-Pinto, J. Zhang, T.J.J. Blanck, F. Xu, Cytotoxicity of local anesthetics in human neuronal cells, Anesth. Analg. 108 (3) (2009 Mar) 997–1007.
[29] C. Zhang, P. Phamonvaechavan, A. Rajan, D.Y. Poon, P. Topcu-Yilmaz, D.L. Guyton, Concentration-dependent bupivacaine myotoxicity in rabbit extraocular muscle, J. AAPOS 14 (4) (2010 Aug) 323–327.
[30] A.B. Sarifakioglu, O.U. Yemisci, S.A. Yalbuzdag, P.O. Ciftkaya, N.S. Cosar, Caudaequina syndrome after cesarean section, Am. J. Phys. Med. Rehabil. 92 (2) (2013 Feb) 179–182.
[31] X. Capdevila, P. Pirat, S. Bringuier, E. Gaertner, F. Singelyn, N. Bernard, O. Choquet, H. Bouaziz, F. Bonnet, French Study Group on Continuous Peripheral NerveBlocks, Continuous peripheral nerve blocks in hospital wards after orthopedic surgery: a multicenter prospectiveanalysis of the quality of postoperative analgesia and complications in 1,416 patients, Anesthesiology 103 (5) (2005 Nov) 1035–1045.
[32] P.W. Benoit, A. Yagiela, N.F. Fort, Pharmacologic correlation between local anestheticinducedmyotoxicity and disturbances of intracellular calcium distribution, Toxicol. Appl. Pharmacol. 52 (2) (1980 Feb) 187–198.

[33] C.H. Cherng, C.S. Wong, C.T. Wu, C.C. Yeh, Intramuscular bupivacaine injection dose-dependently increases glutamate release and muscle injury in rats, Acta Anaesthesiol. Taiwanica 48 (1) (2010 Mar) 8–14.
[34] C. Plank, P. Hofmann, M. Gruber, G. Bollwein, B.M. Graf, W. Zink, T. Metterlein, Modification of bupivacaine-induced myotoxicity with dantrolene and caffeine in vitro, Anesth. Analg. 122 (2) (2016 Feb) 418–423.
[35] W.J. Genovese, Laser de baixa intensidade: aplicações terapêuticas em odontologia, Ed. Santos, São Paulo, 2007.
[36] A.M. Shirani, N. Gutknecht, M. Taghizadeh, M. Mir, Low-level laser therapy and myofacial pain dysfunction syndrome: a randomized controlled clinical trial, Lasers Med. Sci. 24 (5) (2009 Sep) 715–720.
[37] F.J. Dias, J.P.M. Issa, A.P.A. Barbosa, P.B. Vasconcelos, L. Watanabe, M. Mizusakilyomasa, Effects of low-level laser irradiation in ultrastructural morphology, and immunoexpression of VEGF and VEGFR-2 of rat masseter muscle, Micron 43 (2012) 237–244.
[38] L.H. Silva, M.T. Silva, R.M. Gutierrez, T.C. Conte, C.A. Toledo, M.S. Aoki, R.E. Liebano, E.H. Miyabara, GaAs 904-nm laser irradiation improves myofiber mass recovery during regeneration of skeletal muscle previously damaged by crotoxin, Lasers Med. Sci. 27 (5) (2012 Sep) 993–1000.
[39] E. Aranha de Sousa, J.A. Bittencourt, N.K. Seabra de Oliveira, S.V. Correia Henriques, L.C. dos Santos Picanço, C.P. Lobato, J.R. Ribeiro, W.L. Pereira, J.C. Carvalho, J.O. da Silva, Effects of a low-level semiconductor gallium arsenide laser on local pathological alterations induced by *Bothrops moojeni* snake venom, Photochem. Photobiol. Sci. 12 (10) (2013 Oct) 1895–1902.
[40] P.A. Borsa, K.A. Larkin, J.M. True, Does phototherapy enhance skeletal muscle contractile function and postexerciserecovery? A systematic review, J. Athl. Train. 48 (1) (2013) 57–67.
[41] M. Mantineo, J.P. Pinheiro, A.M. Morgado, Low-level laser therapy on skeletal muscle inflammation: evaluation of irradiation parameters, J. Biomed. Oct. 19 (9) (2014 Sep) 98002.
[42] C.E.A. de Freitas, R.S. Bertaglia, I.J.V. Junior, E.A. Mareco, R.A.S. Salomão, T.G. de Paula, G.A. Nai, R.F. Carvalho, F.L. Pacagnelli, M. Dal-Pai-Silva, High final energy of low-level gallium arsenide laser therapy enhances skeletal muscle recovery without a positive effect on collagen remodeling, Photochem. Photobiol. 91 (2015) 957–965.
[43] H.L. Liang, H.T. Whelan, J.T. Eells, M.T. Wong-Riley, Near-infrared light via light-emitting diode treatment is therapeutic against rotenone- and 1-methyl-4-phenylpyridinium ion-induced neurotoxicity, Neuroscience 153 (4) (2008 Jun 2) 963–974.
[44] M. Masoumipoor, S.B. Jameie, A. Janzadeh, F. Nasirinezhad, M. Soleimani, M. Kerdary, Effects of 660- and 980-nm low-level laser therapy on neuropathic pain relief following chronic constriction injury in rat sciatic nerve, Lasers Med. Sci. 29 (5) (2014 Sep) 1593–1598.
[45] V. Erthal, P. Nohama, Treatment for neuropathic pain and chronic inflammation using LASER in animal models, Conf. Proc. IEEE Eng. Med. Biol. Soc. 2015 (2015 Aug) 1315–1318.
[46] L.P. Sergio, V.M. Campos, S.C. Vicentini, A.L. Mencalha, F. de Paoli, A.S. Fonseca, Low-intensity red and infrared lasers affect mRMA expression of DNA nucleotide excision repair in skin andmuscle tissue, Lasers Med. Sci. 31 (3) (2016 Apr) 429–435.
[47] X. Zhang, L. Mu, H. Su, S. Sobotka, Locations of the motor endplate band and motoneurons innervating the sternomastoid muscle in the rat, Anat. Rec. (Hoboken) 294 (2) (2011 Feb) 295–304.
[48] E. Minatel, H. Santo Neto, M.J. Marques, Acetylcholine receptors and neuronal nitric oxide synthase distribution at the neuromuscular junction of regenerated muscle fibers, Muscle Nerve 24 (3) (2001 Mar) 410–416.
[49] J. Gottschall, W. Zenker, W. Neuhuber, A. Mysicka, M. Müntener, The sternomastoid muscle of the rat and its innervation. Muscle fiber composition, perikarya and axons of efferent and afferent neurons, Anat. Embryol. (Berl.) 160 (3) (1980) 285–300.
[50] J.H. Wilkinson, Introduccion al diagnostic enzimatico, third ed. EdicionesToray, Buenos Aires, 1965 (310p).
[51] F. Sweat, H. Puchtler, S.I. Rosenthal, Sirius red F3BA as a stain for connective tissue, Arch. Pathol. 78 (1964 Jul) 69–72.
[52] R.A. Walker, Quantification of immunohistochemistry-issue concerning methods utility and semiquantitative assessment I, Histochemistry 49 (2006) 406–410.
[53] J.H. Zar, Biostatistical Analysis, fifth ed. Prentice-Hall, New Jersey, 2009 994.
[54] J.B. McAlvin, G. Reznor, S.A. Shankarappa, C.F. Stefanescu, D.S. Kohane, Local toxicity from local anesthetic polymeric microparticles, Anesth. Analg. 116 (4) (2013 Apr) 794–803.
[55] A.C. Mendonça, C.H. Barbieri, N. Mazzer, Directly applied low intensity direct electric current enhances peripheral nerve regeneration in rats, J. Neurosci. Methods 129 (2) (2003 Oct 30) 183–190.
[56] A.B. Scott, J.M. Miller, K.R. Shieh, Treating strabismus by injecting the agonist muscle with bupivacaine and the antagonist with botulinum toxin, Trans. Am. Ophthalmol. Soc. 107 (2009 Dec) 104–109.
[57] B.M. Carlson, A quantitative study of muscle fiber survival and regeneration in normal, predenervated, and Marcaine-treated free muscle grafts in the rat, Exp. Neurol. 52 (3) (1976 Sep) 421–432.
[58] P.K. Politi, S. Havaki, P. Manta, G. Lyritis, Bupivacaine-induced regeneration of rat soleus muscle: ultrastructural and immunohistochemical aspects, Ultrastruct. Pathol. 30 (6) (2006 Nov–Dec) 461–469.
[59] O. Oz Gergin, K. Yıldız, A. Bayram, L. Sencar, G. Coşkun, A. Yay, C. Bicer, S. Ozdamar, S. Polat, Comparison of the myotoxic effects of levobupivacaine, bupivacaine, andropivacaine: an electron microscopicstudy, Ultrastruct. Pathol. 39 (3) (2015 May) 169–176.
[60] B. Katiriji, M.M. Al Jaberi, Creatine kinase revisited, J. Clin. Neuromuscul. Dis. 2 (3) (2001 Mar) 158–164.
[61] M. Jasińska, J. Owczarek, D. Orszulak-Michalak, The influence of simvastatin at high dose and diltiazem on myocardium in rabbits, the biochemical study, Acta Pol. Pharm. 63 (5) (2006 Sep–Oct) 386–390.
[62] Y. Tonomura, Y. Mori, M. Torii, T. Uehara, Evaluation of the usefulness of biomarkers for cardiac and skeletal myotoxicity in rats, Toxicology 266 (1–3) (2009 Dec 21) 48–54.
[63] G. Reurink, G.J. Goudswaard, M.H. Moen, A. Weir, J.A. Verhaar, J.L. Tol, Myotoxicity of injections for acute muscle injuries: a systematic review, Sports Med. 44 (7) (2014 Jul) 943–956.
[64] C.M.S. Cereda, G.R. Tofoli, L.G. Maturana, A. Piericci, L.A.S. Nunes, M. Franz-Montan, A.L.R. Oliveira, S. Arana, D.R. Araujo, E. Paula, Local neurotoxicity and myotoxicity evalution of cyclodextrin complexes of bupivacaine and ropivacaine, Int. Anesth. Res. Soc. 115 (5) (2012) 1234–1241.
[65] A.M. Zagatto, Ramos S. de Paula, F.Y. Nakamura, F.S. de Lira, R.Á. Lopes-Martins, R.L. de Paiva Carvalho, Effects of low-level laser therapy on performance, inflammatory markers, and muscle damage in young waterpolo athletes: a double-blind randomized, placebo-controlled study, Lasers Med. Sci. 31 (3) (2016 Apr) 511–521.
[66] C.M. França, Santana C. de Loura, C.B. Takahashi, A.N. Alves, A.P. De Souza Mernick, K.P. Fernandes, D. de Fatima Teixeira da Silva, S.K. Bussadori, R.A. Mesquita-Ferrari, Effect of laser therapy on skeletal muscle repair process in diabetic rats, Lasers Med. Sci. 28 (5) (2013 Sep) 1331–1338.
[67] C. Ferraresi, R.V. Dos Santos, G. Marques, M. Zangrande, R. Leonaldo, M.R. Hamblin, V.S. Bagnato, N.A. Parizotto, Light-emitting diode therapy (LEDT) before matches prevents increase in creatine kinase with a light dose response in volleyball players, Lasers Med. Sci. 30 (4) (2015 May) 1281–1287.
[68] M.C. Pereira, C.B. de Pinho, A.R.P. Medrado, Z.A. Andrade, S.R.A. Reis, Influence of 670 nm low-level laser therapyon mast cells and vascular response of cutaneous injuries, J. Photochem. Photobiol. B Biol. 98 (2010) 188–192.
[69] A.N. Alves, K.P. Fernandes, A.M. Deana, S.K. Bussadori, R.A. Mesquita-Ferrari, Effects of low-level laser therapy on skeletal muscle repair: a systematic review, Am. J. Phys. Med. Rehabil. 93 (12) (2014 Dec) 1073–1085.
[70] R.A. Mesquita-Ferrari, M.D. Martins, J.A. Silva Jr., T.D. da Silva, R.F. Piovesan, V.C. Pavesi, S.K. Bussadori, K.P. Fernandes, Effects of low-level laser therapy on expression of TNF-α and TGF-β3 in skeletal muscle during the repair process, Lasers Med. Sci. 26 (3) (2011 May) 335–340.
[71] L. Assis, A.I. Moretti, T.B. Abrahão, V. Cury, H.P. Souza, M.R. Hamblin, N.A. Parizotto, Low-level laser therapy (808 nm) reduces inflammatory response and oxidative stress in rat tibialis anterior muscle after cryolesion, Lasers Surg. Med. 44 (9) (2012 Nov) 726–735.
[72] S.R. Morais, A.G. Goya, Ú. Urias, P.R. Jannig, A.V. Bacurau, W.G. Mello, P.L. Faleiros, S.H. Oliveira, V.G. Garcia, E. Ervolino, P.C. Brum, R.C. Dornelles, Strength training prior to muscle injury potentiates low-level laser therapy (LLLT)-induced muscle regeneration, Lasers Med. Sci. (2016 Dec 1) (Epub ahead of print).
[73] D. Pires, M. Xavier, T. Araújo, J.A. Silva Jr., F. Aimbire, R. Albertini, Low-level laser therapy (LLLT; 780 nm) acts differently on mRNA expression of anti- and pro-inflammatory mediators in an experimental model of collagenase-induced tendinitis in rat, Lasers Med. Sci. 26 (1) (2011 Jan) 85–94.
[74] A.B. Macedo, L.H. Moraes, D.S. Mizobuti, A.R. Fogaça, S. Moraes Fdos, A. Hermes Tde, A. Pertille, E. Minatel, Low-level laser therapy (LLLT) in dystrophin-deficient muscle cells: effects on regeneration capacity, inflammation response and oxidative stress, PLoS One 10 (6) (2015 Jun 17), e0128567.
[75] M. Mantineo, J.P. Pinheiro, A.M. Morgado, Low-level laser therapy on skeletal muscle inflammation: evaluation of irradiation parameters, J. Biomed. Opt. 19 (9) (2014 Sep) 98002.
[76] L. Luo, A. Sun, L. Zhang, X. Li, Y. Dong, T.C. Liu, Effects of low-level therapy on ROS homeostasis and expression of IGF-1 and TGF-β1 in skeletal muscle during the repair process, Lasers Med. Sci. 28 (2013) 725–734.
[77] X.E. Li, L. Zhu, T.C. Liu, Fibrosis inhibition of photobiomodulation promoted regeneration, Photomed. Laser Surg. 31 (10) (2013 Oct) 505–506.
[78] J.M.D. Baptista, V.C.S. Martins, S.K. Pavesi, K.P.S. Bussadori, D.S.P.J. Fernandes, R.A. Mesquita-Ferrari, Influence of laser photobiomodulation on collagen IV during skeletalmuscle tissue remodeling after injury in rats, Photomed. Laser Surg. 29 (2010) 1–7.
[79] FdaR Guerra, C.P. Vieira, M.S. Almeida, L.P. Oliveira, A.A. de Aro, E.R. Pimentel, LLLT improves tendon healing through increase of MMP activity and collagen synthesis, Lasers Med. Sci. 28 (2013 Sep) 1281–1288.
[80] P.C.L. Silveira, L.A. Silva, C.A. Pinho, P.S. Souza, M.M. Ronsani, D. Scheffer, R.A. Pinho, Effects of low-level laser therapy (GaAs) in an animal model of muscular damage induced bytrauma, Lasers Med. Sci. 2013 (28) (2013) 431–436.
[81] A.N. Alves, K.P.S. Fernandes, C.A.V. Melo, R.Y. Yamaguchi, C.M. França, D.F. Teixeira, S.K. Bussadori, F.D. Nunes, R.A. Mesquita-Ferrari, Modulating effect of low level-laser therapy on fibrosis in the repair process of the tibialis anterior muscle in rats, Lasers Med. Sci. 29 (2) (2014 Mar) 813–821.
[82] B.G. Ribeiro, A.N. Alves, L.A. Santos, K.P. Fernandes, T.M. Cantero, M.T. Gomes, C.M. França, D.F. Silva, S.K. Bussadori, R.A. Mesquita-Ferrari, The effect of low-level laser therapy (LLLT) applied prior to muscle injury, Lasers Surg. Med. (2015 Jul 6).
[83] C.C. Alcântara, D. Gigo-Benato, T.F. Salvini, A.L. Oliveira, J.J. Anders, T.L. Russo, Effect of low-level laser therapy (LLLT) on acute neural recovery and inflammation-related gene expression after crush injury in rat sciatic nerve, Lasers Surg. Med. 45 (4) (2013 Apr) 246–252.
[84] M.M. Iyomasa, E.C. Rizzi, J.C. Leão, J.P. Issa, F.J. Dias, Y.C. Pereira, M.J. Fonseca, F.T. Vicentini, I.S. Watanabe, Zymographic and ultrastructural evaluations after low-level laser irradiation on masseter muscle of HRS/J strainmice, Lasers Med. Sci. 28 (3) (2013 May) 777–783.

[85] T. Karu, Primary and secondary mechanisms of action of visible to near-IR radiation on cells, J. Photochem. Photobiol. B 49 (1) (1999 Mar) 1–17.
[86] H. Chung, T. Dai, S.K. Sharma, Y.Y. Huang, J.D. Carroll, M.R. Hamblin, The nuts and bolts of low-level laser (light) therapy, Ann. Biomed. Eng. 40 (2) (2012 Feb) 516–533.
[87] F. Martins, A.C. Rennó, Oliveira Fd, N.P. Minatel, J.A. Bortolin, H.T. Quintana, M.C. Aveiro, Low-level laser therapy modulates musculoskeletal loss in a skin burn model in rats, Acta Cir. Bras. 30 (2) (2015 Feb) 94–99.
[88] C.S. Enwemeka, Intricacies of dose in laser phototherapy for tissue repair and pain relief, Photomed. Laser Surg. 27 (2009) 387–393.